Native defects in undoped semi-insulating CdSe studied by photoluminescence and absorption

D. L. Rosen, Q. X. Li, and R. R. Alfano

Institute for Ultrafast Spectroscopy and Lasers, Physics Department and Electrical Engineering Department,
The City College of New York, New York, New York 10031

Recombination of carriers in semi-insulating undoped CdSe was studied using infrared absorption and both the polarization and excitation power dependence of the photoluminescence spectra. The photoluminescence measurements showed that a deep donor and a shallow-acceptor state dominate the recombination process, which is slightly modified by a conduction-band tail. Polarization studies showed that the shallow-acceptor level is spin split by ~ 1.7 meV, and that the band-tail states do not have the same symmetry as the maximum allowed symmetry of the crystal. The absorption spectra showed indirect absorption from energy levels of the shallow-acceptor defect, including a possible deep level at ~ 1.3 eV. Deep-donor levels of the shallow-acceptor defect may be responsible for high-resistivity undoped CdSe and the self-compensation of p-CdSe.

I. INTRODUCTION

Large-band-gap semiconductors, which include many II-VI compounds, are prime candidates for blue-green lasers, light-emitting diodes, and other optoelectronic systems. The use of these materials in technology is largely impeded by the self-compensation effect, because it often prevents the fabrication of p-n junctions from a semiconductor.[1,2] Self-compensation refers to the fact that some polar semiconductors are naturally n-type (such as ZnSe or CdSe) or p-type (such as ZnTe or Cu_2O) and resist doping by shallow impurities of the opposite type. Two types of mechanisms for self-compensation are the chemical mechanisms, where chemically generated defects compensate the shallow impurity, and the physical mechanisms, where deep energy levels of the shallow dopant prevent the impurity from ionizing. Experimental evidence from this research, using nonlinear luminescence and absorption, shows evidence to support the second type of mechanism of self-compensation in CdSe.

Carrier recombination and defect-related properties of semiconductors have often been studied by nonlinear luminescence and below-gap absorption.[3-15] The energy distribution of recombination centers[3-13] and band tailing[14,15] have been particularly studied by these methods. Models for understanding kinetics have included the two-center recombination model by Klasens,[3,4] the three-center recombination model by Bube,[5] and the quasicontinuous center by Rose.[6] Distinguishing between models is difficult because of uncontrolled native defects, impurity broadening, and symmetry-breaking effects, particularly in CdSe. In this paper we show that the two-center model for recombination, modified by the conduction-band tail, is sufficient to explain the photoluminescence data in undoped semi-insulating CdSe. One of these centers, the shallow-acceptor defect, was further studied by midgap absorption. Symmetry properties of the shallow impurities and band tail were studied by photoluminescence polarization. A deep level in the shallow-acceptor defect was found and considered as possibly contributing to self-compensation in CdSe.

II. METHODS AND MATERIALS

Five undoped samples of CdSe, supplied by Cleveland Crystals, Inc., three made semi-insulating by treatment with Se vapor (samples denoted here by the labels H_1, H_2, and H_3) and two n-type (samples denoted here by the labels L_1 and L_2), were studied by photoluminescence and absorption spectroscopy. Sample H_1 was 2 mm thick, while samples H_2 and H_3 were 1.55 mm thick. Samples H_2 and L_1 had their optical c axes parallel to the surface for polarization studies. The c axis of other samples was perpendicular to the surface. The low-resistivity samples, L_1 and L_2, were only studied by photoluminescence in order to show that their dynamics are different from the dynamics of the high-resistivity samples.

For photoluminescence, the excitation was provided by a Coherent model no. 52 Ar-ion laser at 488 nm, the beam was focused to an intensity of $\sim 10^5$ W/cm^2 at maximum and the excitation power was varied using neutral density filters. The excitation was chopped at 100 Hz and detected by a RCA 7265 photomultiplier tube (PMT) and a Princeton Applied Research model no. HR-8 lock-in amplifier. The linearity of the system was checked using a scatter plate.

For absorption, the light source was an incandescent tungsten lamp and the detector was a PbS cell. The lamp was also chopped and detected by the same lock-in system. The absorption coefficient was calculated at each wavelength, and corrected for reflection at the two surfaces, using values for the index of refraction of CdSe found in the literature.[16]

III. DATA

A. Photoluminescence

At 77 K, the photoluminescence spectra of each sample consisted of two major bands.[17-19] The photoluminescence spectra are displayed in Fig. 1 for the high-resistivity samples at 77 K. The free-carrier band (XH band) which peaked at 682 nm, showed conduction-electron—to—hole (CH) transitions and shallow-donor—
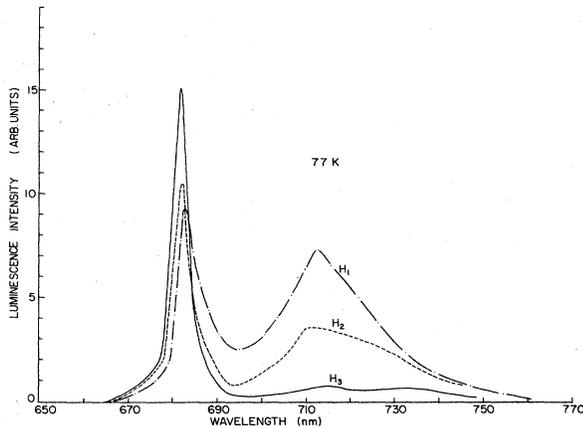
FIG. 1. Luminescence spectra of semi-insulating samples of CdSe (three samples) at 77 K, showing the XH and XA bands. Sample H_1 at 77 K (—·—·—·), sample H_2 at 77 K (— — —), sample H_3 at 77 K (———).

to—hole (DH) transitions. The other broad band (XA band) which peaked at ~720 nm, shows both electron-to-shallow acceptor (CA) and shallow-donor-to-acceptor (DA) transitions. Previous investigators have shown that the CA transitions predominate above 30 K.[19] As the temperature was raised over 200 K, the XA band disappeared due to the ionization of the shallow-acceptor state. At room temperature, the XH band had shifted to 712 nm and broadened as shown in Fig. 2 for the high-resistivity samples. Sample H_3 had a very small uncharged acceptor concentration as shown by the small XA band in Fig. 1 and by its high quantum efficiency (about 100 times the quantum efficiency of H_1 and H_2).

The intensity dependence of the photoluminescence is displayed in Fig. 3 for the XH bands and Fig. 4 for the XA band. The photoluminescence intensity (I_L) as a function of excitation power (I_P) was fitted over two to
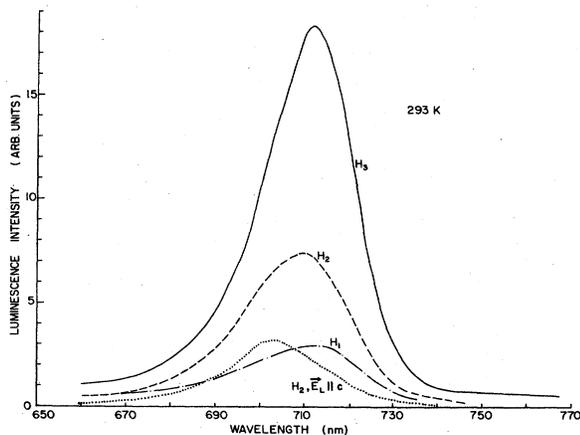
FIG. 2. Luminescence spectra of semi-insulating CdSe at room temperature, showing the XH band. The spectra for H_2 for $E_L||c$ at room temperature is also shown. Sample H_1 (—·—·—·), sample H_2 for total luminescence (— — —), sample H_2 for $E_L||c$ (· · · ·), sample H_3 (———).
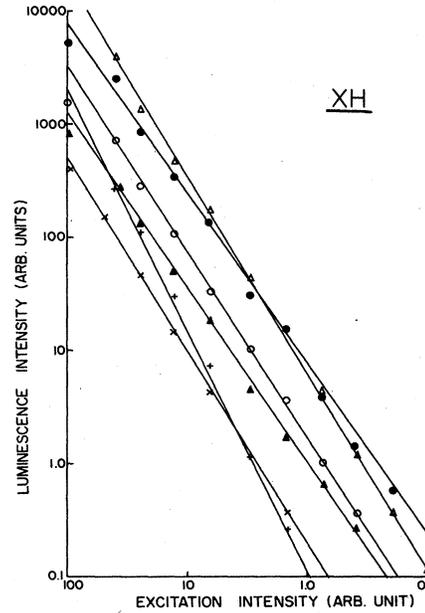
FIG. 3. Intensity of luminescence I_L, as a function of intensity of excitation I_P at the peak of the XH band for different samples at different temperatures. H_1 at 77 K (+), H_1 at 293 K (×), H_2 at 77 K (●), H_2 at 293 K (△), H_3 at 77 K (△), H_3 at 293 K (○).

three decades to a power law according to $I_L \sim I_P^n$ as shown in Figs. 3 and 4 for the semi-insulating samples. The acceptor band was sublinear above a certain intensity, indicating the onset of saturation. We discuss only the sublinear region.
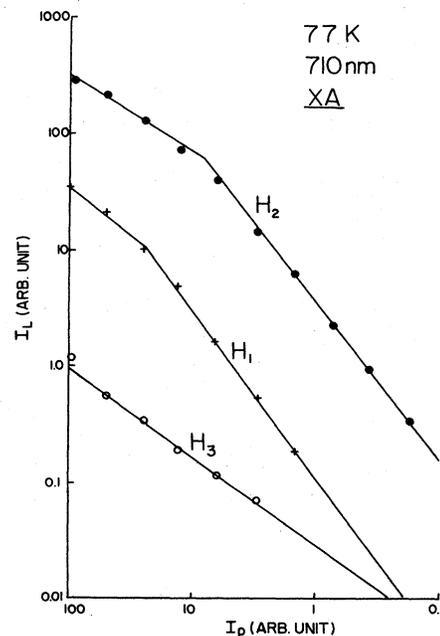
FIG. 4. Intensity of luminescence I_L, as a function of excitation intensity I_p at the peak of the XA band for different samples at 77 K. Sample H_1 (+), sample H_2 (●), sample H_3 (○).

TABLE I. Excitation power laws and models, coded according to system described in Ref. 4.

Sample	Temperature (K)	n	Band	Condition
High-resistivity samples				
H_1	77	2.0	XH	114121
H_1	77	0.8	XA	114121
H_1	293	1.6	XH	221221
H_2	77	1.4	XH	221221
H_2	77	0.8	XA	221221
H_2	293	1.5	XH	221221
H_3	77	1.6	XH	221221
H_3	77	0.7	XA	221221
H_3	293	1.6	XH	221221
Low-resistivity samples				
L_1	77	1.2	XH	
L_1	77	0.9	XA	
L_1	293	1.6	XH	221221
L_2	77	1.2	XH	
L_2	77	0.7	XA	
L_2	293	1.3	XH	

The parameter n was constant to within 5%. This value did not change with polarization or spatial site on the sample. The value of n was different for both bands. Table I shows n for both bands at 77 K and room temperature for each sample. Each n in Table I was measured at the peak wavelength. The XH band was superlinear ($n > 1$) and the XA band was usually sublinear ($n < 1$). The table shows n for the XA band only in the sublinear intensity region. The low-resistivity samples were more linear than the high-resistivity samples, indicating a possible difference in recombination kinetics. This paper concentrates on the high-resistivity CdSe samples, in order to focus on the compensation mechanism. More work will be done on low-resistivity CdSe samples.

The exponent n increased just below band gap in the XH band, for all semi-insulating samples. This increase in n was difficult to measure because the XH luminescence was weak in this region. In order to demonstrate the increase in n for the XH band below band gap, a plot of the ratio

$$R(\lambda) = I_L(2I_p)/I_L(I_p) \tag{1}$$

as a function of photoluminescence wavelength λ was studied, as shown in Fig. 5 for a typical semi-insulating
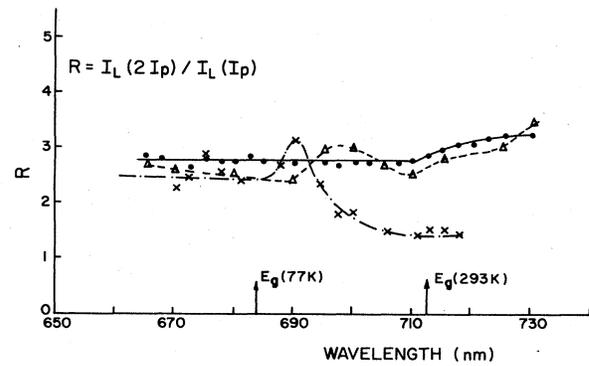
FIG. 5. Ratio $R(\lambda)$ for sample H_2 in the XH band, where $R(\lambda) = I_L(2I_P)/I_L(I_P)$, showing how n increased below the band gap in all cases. At 77 K ($\times$), at 293 K ($\bullet$), at 293 K, $\vec{E}_L || \hat{c}$ ($\triangle$).

sample H_2. Here, $I_L(I_p)$ is the photoluminescence intensity measured with excitation intensity I_p, and $I_L(2I_p)$ is the photoluminescence when the excitation is doubled. The figure shown is the average of four such measurements. The values of R are shown for three situations: total luminescence (mostly $\vec{E}_L \perp \hat{c}$) at 77 K and room temperature, and for polarization parallel to the optical c axis at room temperature (i.e., $\vec{E}_L || \hat{c}$) for sample H_2.

The following salient points should be noted. The increase in R was just below band gap at both temperatures for the total luminescence, indicating the states involved were shallow levels. For $\vec{E}_L || \hat{c}$, there were two maxima, one just below the conduction-electron to A-hole transition and one below the conduction-electron to B-hole transition, while there was only one maximum for the total luminescence. The ratio R in the XA band was usually less than two, indicating sublinearity.

In order to roughly delineate the symmetry properties of the shallow impurity levels and the free carriers, photoluminescence polarization studies of sample H_2 (where the optical axis c was parallel to the surface) were done at 77 K, 200 K, and room temperature. At each temperature, the peak wavelength for the XH band was about 10 nm longer for $\vec{E}_L \perp \hat{c}$ than for $\vec{E}_L || \hat{c}$, consistent with the selection rules already known for a CH transition,[20] while the XA band did not noticeably shift with polarization. The long-wavelength XH tail was about 5 nm longer for the $\vec{E}_L || \hat{c}$ case than for the $\vec{E}_L \perp \hat{c}$ case, as shown in Fig. 2.

TABLE II. Photoluminescence polarization: sample H_2.

Temperature (K)	Band	Wavelength (nm)		Polarization
77	XH	$\perp$	682	22
		$\parallel$	673	
77	XA	$\perp, \parallel$	715	6.5
200	XH	$\perp$	707	3.4
		$\parallel$	697	
200	XA	$\perp, \parallel$	725	3.0
293	XH	$\perp$	715	1.7
		$\parallel$	705	
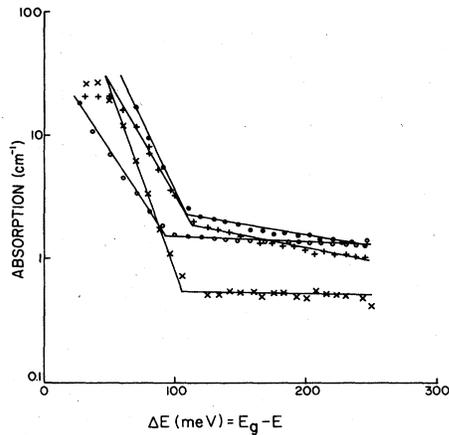
FIG. 6. Near-band-edge absorption α in cm^{-1} as a function of energy below the band gap for two high-resistivity samples, in meV. Indicated is the threshold at ~ 105 meV, and a larger absorption for H_1. H_1 at 77 K (●), H_1 at 293 K (+), H_3 at 77 K, (○), H_3 at 293 K (×).
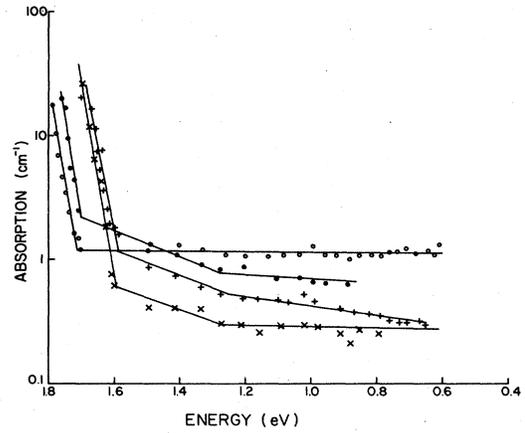
FIG. 7. Absorption α in cm^{-1} as a function of photon energy for two high-resistivity samples, indicating a weak deep-level absorption in H_1 at room temperature, from 0.6 to 1.8 eV. H_1 at 77 K (●), H_1 at 293 K (+), H_3 at 77 K (○), H_3 at 293 K (×).

The two maxima in R and the longer XH tail for $\vec{E}_L||\hat{c}$ both show that the XH luminescence band below band gap is only partially polarized for both A and B holes, unlike the CH luminescence in which $\vec{E}_L\perp\hat{c}$ for the A hole.

The XH band peaked at different wavelengths $\lambda_\perp$ and $\lambda_{||}$, for $\vec{E}_L\perp\hat{c}$ and $\vec{E}_L||\hat{c}$, while $\lambda_\perp=\lambda_{||}$ for the XA band. To correct for this shift, the polarization of each band was defined:

$$p(\lambda)=I_\perp(\lambda+\lambda_\perp-\lambda_{||})/I_{||}(\lambda) . \tag{2}$$

It was found that $p(\lambda)$ was nearly constant for the XA band and the above-band-gap XH band. The wavelengths of the peak intensities and the polarizations of both bands at each temperature are shown in Table II. The polarization of a band is defined in the table as the ratio of the peak intensities for luminescence polarized perpendicular and parallel to the c axis for both XH and XA bands [i.e., $\lambda=\lambda_{||}$ in Eq. (2)]. At 77 K, a second small peak at 682 nm was observed for $\vec{E}_L||\hat{c}$, probably due to the small ($\sim 5°$) collection angle of the experimental geometry. At 200 K, the XH and XA bands overlapped for $\vec{E}_L\perp\hat{c}$. It was determined that none of these effects would significantly effect the polarizations shown. The value of the polarization across the CH band was almost constant if corrected for the peak shift, while the polarization across the XA band was constant with no correction. A salient point of Table II is that both the CH and XA polarization were strongly dependent on temperature.

B. Absorption

The absorption spectra for high-resistivity samples H_1 and H_3 was measured from 0.6 to 1.8 eV and showed two components. The near-band-edge component was measured as a function of energy below band gap and shown in Fig. 6, which is an average of two curves. The first component of absorption showed a threshold at ~ 105 meV, below the band edge, where one would expect shallow-acceptor to conduction-band (AC) transitions. Above this threshold, the absorption curve was fitted to the following square-law dependence of the absorption coefficient α:

$$\alpha(E)=s(E-E_0)^2+b , \tag{3}$$

where E_0 is the threshold, b is the deep-state absorption near the 105-meV threshold, and s is an indirect absorption parameter. Parameters E_0, b, and s are shown in Table III. The threshold showed that the exponential DH tail contributed little to the absorption.

A residue absorption component, which extended all the way to ~ 1.3 eV, changed when the sample was cooled from 293 to 77 K. The absorption to the middle of the gap for both samples, at room temperatures and 77 K, is shown in Fig. 7, where the energy is measured from zero instead of from the band gap. Each curve shows the average of four measurements. This component of absorption had an observable threshold of ~ 1.3 eV, except for H_3 at 77 K. The slope of each component was almost indepen-

TABLE III. Near-band-edge absorption parameters.

Sample	Temperature (K)	Threshold (meV)	s (meV^{-2} cm^{-1})	b (cm^{-1})
H_1	77	115	5.9×10^{-3}	2.2
H_1	293	110	6.1×10^{-3}	2.5
H_3	77	90	4.6×10^{-3}	1.5
H_3	293	110	5.4×10^{-3}	0.5

dent of temperature, though the value of the absorption was not independent of temperature.

IV. RESULTS AND DISCUSSION

A. Photoluminescence

The exponents n, shown in Table I, suggest the type of recombination process which occurs in each sample. A salient point is that the XA band was sublinear above a breaking-point intensity, similar to results found in CdS,[7,8] while the XH band was always more than linear. This breaking-point intensity in the XA band, predicted by all nonlinear luminescence theories, indicates that above this intensity the acceptor level saturates by trapping free carriers and thus plays an important role in recombination. This paper focuses on the sublinear region, in order to identify recombination pathways. In all cases, except for L_1 at 293 K, the XH band for the high-resistivity samples was much more nonlinear than the XH band of the low-resistivity samples, showing a difference in recombination mechanisms. The exponent n was nearly 1.5 or 2 in the XH band of the semi-insulating samples, while the value of n was usually 1.2 for the low-resistivity samples. Thus, the dynamics of the high-resistivity samples are probably related to the compensation mechanism of the crystal. As stated above we will concentrate on studying the high-resistivity samples in this paper. Further work is being done on the undoped low-resistivity samples.

The results for the semi-insulating samples were interpreted in terms of recombination-level theory.[3-6] The nonlinearity indicated that the excitation is in the quasi-Fermi-level region. Three models were considered; the one- and two-center model by Klasens,[3,4] the three-center model by Cardon and Bube,[5] and the quasi-continuous-center model by Rose.[6] The three-center model by Bube predicts nonpower-law behavior for the luminescence, in which the luminescence rises faster than a square law, which contradicts the data. The quasi-continuous-center model predicts power laws between 1 and 2 for the XH band, and a Fermi level in the impurity-state region.[6] However, no sharp discontinuity in R (indicating a Fermi level) was seen in the sublinear XA bands, as shown in Fig. 5, and this model does not explain why n in the XH bands of the semi-insulating (SI) samples came near 1.5 and 2. The one- or two-center model by Klasens and Duboc assumes two discrete energy levels, and appears to fit most of the data. This model must be slightly modified by the conduction-band tail. In the two-center model, the different conditions and their power laws are coded. Table I indicates the appropriate condition for each sample, coded as in the literature,[4] taking into account other factors which will be discussed.

The notation of the two-center model in Ref. 4 will now be reviewed. One impurity level A is below the dark Fermi level, while H is an impurity level which is above the dark Fermi level. We assumed, in the experimental analysis, that the shallow acceptor responsible for the XA band was A, and that some nonluminescent deep donor was H. The concentration of total A centers, A centers

filled with electrons and A centers empty of electrons are designated a, a^0, and a^+, respectively. Similarly, the concentration of H centers, H centers filled with electrons, and empty H centers are designated h, h^-, and h^0. Free electrons and free holes have concentrations n and p. The above-gap excitation laser has an intensity U, luminescence from free electron to A has intensity $I \sim na^+$, the luminescence from H to valence band has intensity $R \sim ph^-$, and the free electron recombining with free hole luminescence has intensity $F \sim np$. The nonradiative rates C, L, E, and B belong to the free-hole to occupied-A-center transition, the thermal release of holes from empty A centers, the capture of free electrons by H levels, and the thermal release of electrons from occupied H levels, respectively. This simplified model assumes that A and H are two discrete levels, and does not consider the effect of the conduction-band tail or very shallow donors, although our experiments indicated they have a small effect in SI CdSE.

Each concentration, and also the luminescence associated with the concentrations, depends as a power on the excitation intensity U (i.e., $n \sim U^x$, $a^+ \sim U^y$, so $I \sim U^{x+y}$), where the power law depends on the particular conditions of the experiment. For the simplified two-center model, each experimental condition is coded according to the following set of simplified equations:

$$
\begin{array}{llll}
(1) \ a = a^0, & (2) \ a = a^+ , \\
(1) \ h = h^0, & (2) \ h = h^- , \\
(1) \ a^+ = h^-, & (2) \ a^+ = n, & (3) \ h^- = p, & (4) \ n = p , \\
(1) \ U \sim I, & (2) \ U \sim R , \\
(1) \ C = L, & (2) \ C \sim I , \\
(1) \ E = B, & (2) \ E \sim R ,
\end{array} \tag{4}
$$

The simplified equations for single-center models are similar and will not be discussed.

All situations which can occur and which are possible combinations of the six equations above, one out of each row, are indicated by a code number consisting of six digits. Each digit corresponds to one row of the set of equations (4) and indicates which equation of the corresponding row is chosen. Each condition has its own power laws, enumerated in Ref. 4. Although each power law holds over many orders of magnitude in U, each coded condition shows a "breaking-point" transition into another coded condition at fixed values of U. The fact that the XA band showed a breaking point in Fig. 4 while the XH band in Fig. 3 did not show a breaking point supports the existence of a deep-level H which saturates faster than the shallow-acceptor A saturates, but no quantitative analysis of the breaking point was done.

Before analyzing the data on the actual samples, an illustration of the Klasens theory will now be described. Consider a sample at some intermediate pumping intensity U in which condition 111212 applies. Using the set of

equations (4), it is seen that $a = a^0$, $h = h^0$, $a^+ = h^-$, $U \sim R$, $C = L$, and $E \sim R$. Using Table 2 in Ref. 4, it is immediately seen that $I \sim U^{1.5}$, $n \sim U$, $p \sim U^{0.5}$, and $h^- \sim U^{0.5}$. Using the formula for free-carrier luminescence $F \sim np$, it is seen that $F \sim U^{1.5}$. Hence, the power law for both the free-carrier luminescence F and the acceptor luminescence I in terms of pump intensity U is 1.5 under condition 111212.

Condition 111212 is valid only over a limited range in U, from U_i to U_f, where breaking points U_i and U_f are determined by h, a, and other parameters. According to Fig. 14 of Ref. 4, for certain values of the parameters, for U below U_i condition 111211 is valid (where $F \sim U$), from U_i to U_f condition 111212 is valid $(F \sim U^{1.5})$, and above U_f condition 211212 is valid (where $F \sim U^{2.0}$). However, U_f can be much larger than U_i so $F \sim I \sim U^{1.5}$ can be valid over many orders of magnitude. Physically, this situation is descriptive of a sample controlled by a deep acceptor A where the higher the intensity U, the fewer electrons in H. In this case, U_i indicates the transition of H from an electron trap to a recombination center, while U_f indicates the emptying of center A of electrons at higher intensity excitation. Klasens only calculated the breaking points for special cases, none of which included the conditions of the actual samples, so no quantitative analysis of these breaking points were done.

This theory is now applied to the samples of undoped SI CdSe studied. The sublinearity of the XA band indicates that the shallow-acceptor defect acts as one of the discrete recombination levels. The ratio R was analyzed to find out how the band tail affects recombination. The rise below band gap indicates that the conduction band has a tail of localized states. The band tail itself is not a main recombination center. The deviations of n in the XA band from 0.5 or 1, the anomalous behavior of the n-type samples, and the rise below band gap of the XH band suggest that the two-center theory may be perturbed by the tailing of the conduction band (i.e., by shallow donor to acceptor transitions), which raises the tail's power law slightly above the Klasens-Duboc law. Thus the rise below band gap is assumed to indicate that when the free conduction electrons have a power law of 0.5, the respective localized tail states have a power law of ~ 0.7. This condition would result in n for the DA transitions being ~ 0.7 instead of 0.5, as is seen for the XA band. This suggests that DA transitions predominate over CA transitions in the XA band. We assume the shallow donors are perturbed more than the shallow acceptors, because the shallower donors have a much smaller binding energy than the acceptors.

With these assumptions the kinetics in the different samples at the different temperatures can be deduced from the data. Therefore, each crystal can be characterized according to Ref. 4. Let us now consider the case at 77 K for H_2 and H_3. Because no single-level model in Ref. 4 predicts both $n = 1.5$ and a sublinear XA band, we deduce a deep-donor state in addition to the shallow acceptor. There are two conditions in Ref. 4 under which the free-carrier band can have n as 1.5 and the recombination center have $n < 1$. In the first condition (113222), the hole concentration p is proportional to $I_p^{0.5}$, while in the

second condition (221221) the conduction-electron concentration n is proportional to $I_p^{0.5}$. In the first model, using the assumption about the tail previously stated, the band-tail luminescence has an n of 1.2 while in the second, the band tail has an n of 1.7. This second condition (221221) is more consistent with the increase in R below band gap which is shown in Fig. 5. Therefore, the second condition appears appropriate to H_2 and H_3 at this intensity. Under this condition, the deep donors and acceptors have an equal density (plausible for a compensated sample), the deep donors are occupied while the acceptors are empty, the donors are in thermal equilibrium with the conduction band, the acceptor does not release holes, and all holes are recombined through donors. In other words, H_2 and H_3 were slightly n-type CdSe samples highly compensated with acceptor impurities. The exponent n_{XH} for H_1 was 2 at 77 K and 1.6 at room temperature, while n_{XA} at 77 K was 0.8. Sample H_1 was compensated so the number of donors may be equal to the number of acceptors. Therefore, the most plausible model for recombination of sample H_1 at 77 K is Klasens model 114121, where all acceptors and donors are empty, the number of conduction electrons is equal to the number of holes, and all holes are captured by acceptors and not released. Sample H_3 can be considered low in acceptor concentration because its XH band intensity was much stronger than its XA band intensity $(I_{\text{XH}}/I_{\text{XA}} \sim 100)$ relative to H_1 and H_2 $(I_{\text{XH}}/I_{\text{XA}} \sim 0.3)$, and because its XH band intensity was much stronger than that of the other two samples, by a factor of 100. Sample H_1 had the largest acceptor concentration, as shown by the XA band intensity in Fig. 1. The results for all compensated CdSe samples were interpreted as indicating different conditions in the theory, as shown in the Table I. Each condition indicates the existence of a deep donor working with the shallow acceptor.

The noncompensated samples were nearly linear at 77 K, perhaps due to the absence of shallow acceptors. However, for L_1, n_{CH} increases to 1.6 at room temperature and the band tail n increases to 2, which may indicate that L_2 is slightly compensated, with acceptor and donor density both nearly equal and small. At high temperature, ionization of acceptors leads to condition 221221 in sample L_1.

While polarization studies by themselves are insufficient for the purpose of reaching an unequivocal conclusion about the nature of the centers, the polarization data together with additional experimental results can be used to select between plausible models. The nonlinear luminescence data described in this paper suggest the use of modified Lambe-Klicke model for the tail luminescence and a modified Schoen-Klasens model for the XA luminescence.[21,22]

The two maxima in R for $\vec{E}_L || \hat{c}$, shown in Fig. 4, and the width of the $\vec{E}_L || \hat{c}$ luminescence tail, shown in Fig. 2, showed that the DH luminescence for A holes and B holes is only partially polarized. The shift in peak for the XH band verifies that the CH luminescence is completely polarized $\vec{E}_L \perp \hat{c}$, if the hole is in the A band.[20] Therefore, the band tail did not have the maximum allowed symmetry of the intrinsic crystal, which is the simplest assump-

tion one could make about the donor in Lambe-Klicke theory.[21] The symmetry of the localized states of the tail was broken by their inhomogeneous environment (i.e., stacking faults, heavy compensation, or surface broadening as in the case of ZnO.)[22]

The polarization in Table II was analyzed by the Schoen-Klasens model. The polarization of the XH band was strongly temperature dependent, consistent with an A-B band splitting of 27 meV shown by the peak shift. Schoen and Klasens proposed four plausible models for the shallow-acceptor level: two single-center models, a spin-split model with each level empty of electrons, and a spin-split model with both acceptor levels full of electrons. The table shows a temperature dependence on the XA band, which eliminates the first three models. The shallow acceptor is therefore a spin-split level occupied with electrons, consistent with Klasens-Duboc model 221221 shown in Table I. The absence of a peak shift in the XA band and the weak temperature dependence of the XA band (compared to the XH band) may indicate a splitting of the acceptor level much less than that of the free holes, suggesting different symmetry-breaking mechanisms for each, as in the case of ZnO:Cu. Using the formula[22] for polarization p,

$$p = a \exp(\gamma/kT) , \qquad (5)$$

we find that γ is ~ 15 meV for the holes (consistent with the 27-meV peak shift) and ~ 1.7 meV for the acceptor. More work is being done is resolve and explain the small shallow-acceptor level spin splitting.

B. Absorption

In order to further study the transitions of the shallow-acceptor defect, absorption spectra of two crystals (H_1 and H_3) were measured near band gap (Fig. 6) and all the way to 0.6 eV (Fig. 7) at 77 and 293 K. The threshold at 105 meV below band edge, shown in Fig. 5 and Table II, probably indicates transitions from the shallow-acceptor level to the conduction-band continuum (AC).[9−15] Sample H_1 showed a much larger absorption than H_3, consistent with the higher acceptor concentration in H_1 shown by the photoluminescent XA band intensity in Fig. 1. The threshold E_0 shown in Table III, averaging 105 meV, indicated the binding energy of the shallow-acceptor level. Assuming an indirect AC transition, as in Eq. (2), parameters s and b characterize the shallow-acceptor level and deeper impurity states. Deep levels of the samples were investigated down to 30% of the energy gap ($E_g \approx 1.7$ eV), as shown in Fig. 7. The deep-level absorption changed with increasing temperature, as shown in Fig. 6 and Table III (parameter b). If this deep level was not associated with the shallow acceptor, it would not change because its binding energy is much larger than $k_B T$. A threshold of ~ 1.3 eV, seen in all samples except H_3 at 77 K, was tentatively identified with this state. This state may be a deep-donor level belonging to the same defect as the shallow acceptor. Work on thicker samples of CdSe is being done to resolve this deep state.

The probable trapping of conduction electrons by the
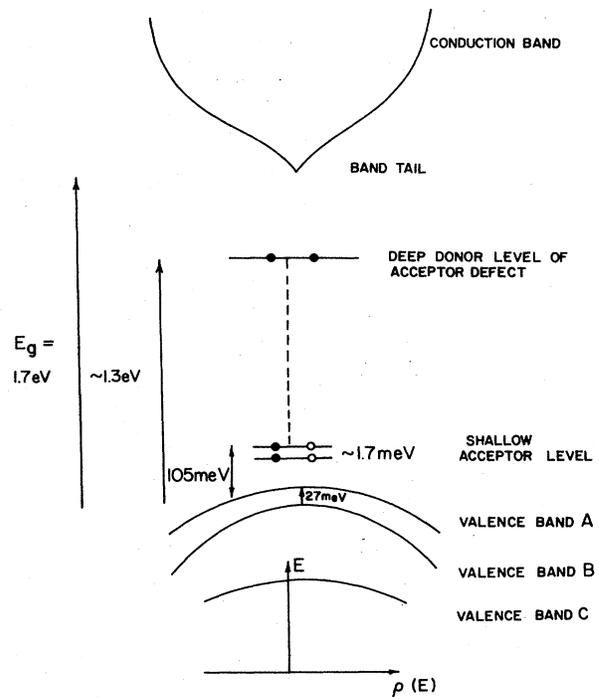
FIG. 8. Proposed energy-level diagram of undoped CdSe, showing the possible different phenomena discussed.

acceptor and the absence of p-type CdSe suggest that this deep level of the acceptor may play an important role in high-resistivity undoped CdSe and in the autocompensation of CdSe. It has been suggested that the shallow-acceptor defect in naturally n-type materials has a deep-donor level which traps electrons.[1,2,23,24] The deep level at ~ 1.3 eV may be this donor level. The value 1.3 eV agrees with the theoretical value predicted by Kobayashi et al.[2] for an antisite Se atom. Further work on the electronic structure of acceptors and relaxation kinetics may add supporting evidence for the physical models of self-compensation.

V. CONCLUSION

Native defects in CdSe have been investigated by nonlinear luminescence and subgap absorption. The recombination dynamics have been shown to be possibly dominated by charge states of the shallow-acceptor defect and a band tail. The acceptor defect contributes to autocompensation in CdSe by trapping conduction electrons instead of releasing holes. The shallow-acceptor level shows very small spin splitting. A possible energy-level diagram of undoped CdSe is shown in Fig. 8.

ACKNOWLEDGMENTS

[1]G. Mandel, Phys. Rev. **134**, A1073 (1964).

[2]Akiko Kobayashi, Otto E. Sankey, and John D. Dow, Phys. Rev. B **28**, 946 (1983).

[3]H. A. Klasens, W. Ramsden, and C. Quantie, J. Opt. Soc. Am. **38**, 60 (1948).

[4]H. A. Klasens, J. Phys. Chem. Solids **7**, 175 (1958).

[5]Felix Cardon and R. H. Bube, J. Appl. Phys. **35**, 7344 (1964).

[6]A. Rose, *Concepts in Photoconductivity and Allied Processes* (Interscience, New York, 1963).

[7]G. Diemes, G. J. van Gurys, and H. J. G. Meyer, Physica (Utrecht) **23**, 987 (1957).

[8]R. Braunstein and N. Ockman, Phys. Rev. **134**, A499 (1964).

[9]E. J. Johnson and H. Y. Tan, Phys. Rev. **139**, A1991 (1965).

[10]B. Tell, J. Appl. Phys. **41**, 3789 (1970).

[11]M. D. Sturge, Phys. Rev. **127**, 768 (1962).

[12]G. B. Stringfellow and R. H. Bube, Phys. Rev. **171**, 903 (1968).

[13]D. Redfield and Martin A. Afromowitz, Appl. Phys. Lett. **11**, 138 (1967).

[14]N. R. Kulish, A. E. Maznichenko, and L. M. Rulakh, Fiz. Tekh. Poluprovodn. **14**, 695 (1980) [Sov. Phys.—Semicond. **14**, 409 (1980)].

[15]A. V. Bazhenov and Y. A. Osip'Yan, Fiz. Tverd. Tela **22**, 991 (1980) [Sov. Phys.—Solid State **22**, 579 (1980)].

[16]N. I. Vitrikhovsky, L. F. Gudimenho, O. P. Maznichenko, V. N. Malinko, E. V. Pidlisnii, and S. F. Terekhova, Ukr. Fiz. Zh. (Russ. Ed.) **12**, 796 (1967).

[17]W. Wardzynski and B. Wojtowicz-Natanson, Proceedings of the International Symposium on Radiative Recombination, Paris, 1960 (unpublished), p. 287.

[18]B. Wojtowicz-Natanson and F. Zahrzewski, Phys. Status Solidi **11**, 873 (1965).

[19]V. V. Dyakin, M. A. Rizakhanov, N. N. Khilomova, and M. K. Sheinkman, Fiz. Tekh. Poluprovodn. **14**, 691 (1980) [Sov. Phys.—Semicond. **14**, 407 (1980)].

[20]H. Yoshida, H. Saho, and S. Shihonoya, J. Phys. Soc. Jpn. **40**, 881 (1981).

[21]J. L. Birman, Proceedings of the International Conference on Luminescence, Budapest, Hungary, 1966 (unpublished), p. 919.

[22]J. L. Birman, J. Electrochem. Soc. **107**, 409 (1960).

[23]M. R. Lorenz, B. Segall, and H. H. Woodbury, Phys. Rev. **134**, A751 (1964).

[24]F. T. Smith, Solid State Commun. **8**, 263 (1970).